

Condition on the Kohn–Sham kinetic energy and modern parametrization of the Thomas–Fermi density

Donghyung Lee,^{1,a)} Lucian A. Constantin,² John P. Perdew,² and Kieron Burke¹

¹*Department of Chemistry, University of California, Irvine, California 92697, USA*

²*Department of Physics and Quantum Theory Group, Tulane University, New Orleans, Louisiana 70118, USA*

(Received 10 October 2008; accepted 10 December 2008; published online 20 January 2009)

We study the asymptotic expansion of the neutral-atom energy as the atomic number $Z \rightarrow \infty$, presenting a new method to extract the coefficients from oscillating numerical data. Recovery of the correct expansion yields a condition on the Kohn–Sham kinetic energy that is important for the accuracy of approximate kinetic energy functionals for atoms, molecules, and solids. For example, this determines the small gradient limit of any generalized gradient approximation and conflicts somewhat with the standard gradient expansion. Tests are performed on atoms, molecules, and jellium clusters using densities constructed from Kohn–Sham orbitals. We also give a modern, highly accurate parametrization of the Thomas–Fermi density of neutral atoms. © 2009 American Institute of Physics. [DOI: 10.1063/1.3059783]

I. INTRODUCTION

Ground-state Kohn–Sham (KS) density functional theory (DFT) is a widely used tool for electronic structure calculations of atoms, molecules, and solids,¹ in which only the density functional for the exchange–correlation energy, $E_{XC}[n]$, must be approximated. But a direct, orbital-free DFT could be constructed if only the noninteracting kinetic energy T_S were known sufficiently accurately as an explicit functional of the density.² Using it would lead automatically to an electronic structure method that scales linearly with the number of electrons N (with the possible exception of the evaluation of the Hartree energy). Thus the KS kinetic energy functional is something of a holy grail of density functional purists, and interest in it was recently revived.³

In this work, we exploit the “unreasonable accuracy” of asymptotic expansions,⁴ in this case for large neutral atoms, to show that there is a very simple condition that approximations to T_S must satisfy, if they are to attain high accuracy for total energies of matter. By matter, we mean all atoms, molecules, and solids that consist of electrons in the field of nuclei, attracted by a Coulomb potential. The condition is to recover the (known) asymptotic expansion of $T_S/Z^{7/3}$ for neutral atoms, in powers of $Z^{-1/3}$. By careful extrapolation from accurate numerical calculations up to $Z \sim 90$, we calculate the coefficients of this expansion. We find that the usual gradient expansion, derived from the slowly varying gas, but applied to essentially exact densities, yields only a good approximation to these coefficients. Thus, all new approximations should either build in these coefficients, or be tested to see how well they approximate them. We perform several tests, using atoms, molecules, jellium surfaces, and jellium spheres, and analyze two existing approximations. In Ref. 5, a related method was used to derive the gradient coefficient in modern generalized gradient approximations (GGAs) for exchange. Given this importance of $N=Z \rightarrow \infty$ as a condition

on functionals, we revisited and improved upon the existing parametrizations of the neutral-atom Thomas–Fermi (TF) density. The second-half of the paper is devoted to testing its accuracy.

II. THEORY AND ILLUSTRATION

For an N -electron system, the Hamiltonian is

$$\hat{H} = \hat{T} + \hat{V}_{\text{ext}} + \hat{V}_{\text{ee}}, \quad (1)$$

where \hat{T} is the kinetic energy operator, \hat{V}_{ext} is the external potential, and \hat{V}_{ee} is the electron–electron interaction, respectively. The electron density $n(\mathbf{r})$ yields $N = \int d^3r n(\mathbf{r})$, where N is the particle number.

To explain asymptotic exactness, we (re)introduce the ζ -scaled potential⁶ (which is further discussed in Ref. 7), given by

$$v_{\text{ext}}^{\zeta}(\mathbf{r}) = \zeta^{4/3} v_{\text{ext}}(\zeta^{1/3} \mathbf{r}), \quad N \rightarrow \zeta N, \quad (2)$$

where $v_{\text{ext}}(\mathbf{r})$ is the external potential and the TF expectation value is $V_{\text{ext}}^{\zeta}[n] = \zeta^{7/3} V_{\text{ext}}[n]$. In this ζ -scaling scheme, nuclear positions \mathbf{R}_{α} and charges Z_{α} of molecules are scaled into $\zeta^{-1/3} \mathbf{R}_{\alpha}$ and ζZ_{α} , respectively. In a uniform electric field $\mathcal{E} \rightarrow \zeta^{5/3} \mathcal{E}$. For neutral atoms, scaling ζ is the same as scaling Z , producing an asymptotic expansion for the total energy of neutral atoms,^{4,8–11}

$$E = -c_0 Z^{7/3} - c_1 Z^2 - c_2 Z^{5/3} + \dots, \quad (3)$$

where $c_0 = 0.768\,745$, $c_1 = -1/2$, $c_2 = 0.269\,900$, and Z is the atomic number. This large Z -expansion gives a remarkably good approximation to the Hartree–Fock energy of the neutral atoms, with less than a 10% error for H and less than 0.5% error for Ne. By the virial theorem for neutral atoms $T = -E$ and $T \approx T_S$ to this order in the expansion (since the correlation energy is roughly $\sim Z$). Hence, the noninteracting kinetic energy has the following asymptotic expansion.

$$T_S = c_0 Z^{7/3} + c_1 Z^2 + c_2 Z^{5/3} + \dots. \quad (4)$$

^{a)}Electronic mail: donghyul@uci.edu.

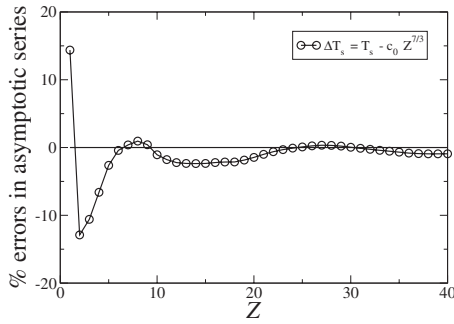


FIG. 1. Percentage error between $c_1 Z^2 + c_2 Z^{5/3}$ and $\Delta T_S = T_S - c_0 Z^{7/3}$.

We say that an approximation to the kinetic energy functional is *asymptotically exact* to the p th degree if it can reproduce the exact c_0, c_1, \dots, c_p . The three displayed terms in Eq. (3) constitute the second-order asymptotic expansion for the total energy of neutral atoms, and we expect that this asymptotic expansion is a better starting point for constructing a more accurate approximation to the kinetic energy functional than the traditional gradient expansion approximation (GEA).

The leading term in Eq. (4) is given exactly by a local approximation to T_S (TF theory), but the leading *correction* is due to higher-order quantum effects, and only approximately given by the gradient expansion evaluated on the exact density. However, these coefficients are *vital* to finding accurate kinetic energies. Since we know that $c_0 Z^{7/3}$ becomes exact in a relative sense as $N=Z \rightarrow \infty$, we define $\Delta T_S = T_S - c_0 Z^{7/3}$ and investigate ΔT_S as a function of Z . How accurate is the asymptotic expansion for ΔT_S ? In Fig. 1, we evaluate T_S for atoms (see Sec. III for details) and plot the percentage error in ΔT_S , for all atoms and the asymptotic series with just two terms. The series is incredibly accurate, with only a 13% error for $N=2$ (He), and 14% for $N=1$. Thus, any approximation that reproduces the correct asymptotic series (up to and including the c_2 term) is likely to produce a highly accurate T_S .

To demonstrate the power and the significance of this approach, we apply it directly to the first term (where the answer is already known but perhaps not yet fully appreciated in the DFT community). Using any (all-electron) electronic structure code, one calculates the total energies of atoms for a sequence running down a column in the periodic table. By sticking with a specific column, one reduces the oscillatory contributions across rows, and the alkali-earth column yields the most accurate results. By then fitting the resulting curve of $T_S/Z^{7/3}$ as a function of $Z^{-1/3}$ to a parabola, one finds $c_0=0.7705$. Now assume one wishes to make a local density approximation (LDA) to T_S , but knows nothing about the uniform electron gas. Dimensional analysis (coordinate scaling) yields¹²

$$T^{(0)}[n] = A_S I, \quad I = \int d^3 r n^{5/3}(\mathbf{r}), \quad (5)$$

but does not determine the constant, A_S . A similar fitting of I , based on the corresponding self-consistent densities, gives a leading term of $0.2677Z^{7/3}$, yielding $A_S=2.868$. Thus we

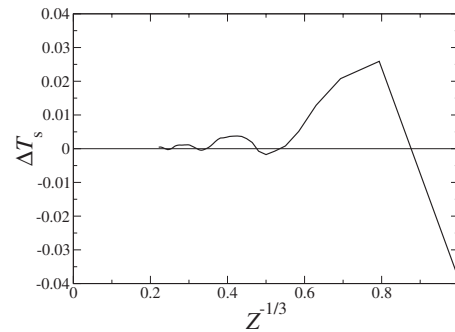


FIG. 2. Difference between $T_S/Z^{7/3}$ and $c_0 + c_1 Z^{-1/3} + c_2 Z^{-2/3}$ as a function of $Z^{-1/3}$.

have deduced the local approximation to the noninteracting kinetic energy.

A careful inspection of the above argument reveals that the uniform electron gas is never mentioned. As N grows, the wavelength of the majority of the particles becomes short relative to the scale on which the potential is changing, loosely speaking, and semiclassical behavior dominates. The local approximation is a universal semiclassical result, which is exact for a uniform gas simply because that system has a constant potential. On the basis of that argument, we know that $A_S = (3/10)(3\pi^2)^{2/3} = 2.871$, demonstrating that (for this case) our result is accurate to about 0.1%. This argument tells us that the reliability of the local approximation is no indicator of how rapidly the density varies. That this argument is correct for neutral atoms was carefully proven by Lieb and Simon¹³ in 1973 and later generalized by Lieb⁶ for all matter.

The focus of the first part of this paper is on the remaining two known coefficients (c_1 and c_2) and how well the GEA performs for them. We evaluate those gradient terms by fitting asymptotic series and find that the traditional gradient expansion does well, but is not exact. From this information, we develop a modified gradient expansion approximation that reproduces the correct asymptotic coefficients c_1 and c_2 , merely as an illustration of the power of asymptotic exactness. We test it on a variety of systems, finding the expected behavior.

In Sec. V, we present a parametrization of the TF density, which is more accurate than previous parametrizations. The TF density has a simple scaling with Z and becomes relatively exact and slowly varying for a neutral atom as $Z \rightarrow \infty$, breaking down only near the nucleus and in the tail. We compare various quantities of our parametrization with exact values and earlier parametrizations and analyze the properties of the TF density.

III. LARGE Z METHODOLOGY

We begin with a careful methodology for extracting the asymptotic behavior from highly accurate numerical calculations. Fully numerical DFT calculations were performed using the OPMKS code¹⁴ to calculate the total energies of neutral atoms using ‘exact exchange’. This is simply minimizing the Hartree–Fock energy, subject to the constraint of a multiplicative potential.¹⁵ The spin-density functional version of T_S has been used for all systems.¹⁶ We refer throughout to these

TABLE I. The coefficients in the asymptotic expansion of the KS kinetic energy and various local and semilocal functionals. The fit was made to $Z = 24$ (Cr), 25 (Mn), 30 (Zn), 31 (Ga), 61 (Pm), and 74 (W). The functionals of the last two rows are defined in Sec. IV.

	c_1	c_2
Exact	-0.5000	0.2699
T_S	-0.5000	0.2702
T^{TF}	-0.6608	0.3854
$T^{(2)}$	0.1246	-0.0494
$T^{(4)}$	0.0162	0.0071
T^{GEA2}	-0.5362	0.3360
T^{GEA4}	-0.5200	0.3431
T^{GGA^a}	-0.5080	0.2918
T^{LmGGA^a}	-0.5089	0.3174

^aSee Sec. IV.

as the KS results, and none of our analysis depends on which approximation we use. The coefficients c_0 , c_1 , and c_2 are the same over a wide range of approximations from exact exchange-correlation to local-density exchange.

To attain maximum accuracy for c_1 and c_2 , we need to suppress the oscillations that come at the same order as the next term, $c_3 Z^{4/3}$. Consider first the KS results (T_S). We investigate the differences between $T_S/Z^{7/3}$ and $c_0 + c_1 Z^{-1/3} + c_2 Z^{-2/3}$ in Fig. 2. We extract six data points [$Z=24$ (Cr), 25 (Mn), 30 (Zn), 31 (Ga), 61 (Pm), and 74 (W)], which have the smallest differences, i.e., nearest to where the curve crosses the horizontal axis. We then make a least-squares fit with a parabolic form in $Z^{-1/3}$, ignoring the oscillation term,

$$\frac{T_S}{Z^{7/3}} = 0.768\,745 + c_1 Z^{-1/3} + c_2 Z^{-2/3}. \quad (6)$$

Effectively, we solve two linear equations for c_1 and c_2 . We explicitly include $c_0=0.768\,745$, since we do not have enough data points to extract c_0 accurately, especially in the region $Z^{-1/3} < 0.2$. It is important to control the behavior of the fitting line at $Z \rightarrow \infty$. This fitting yields an accurate estimate of $c_1 = -0.5000$ and $c_2 = 0.2702$, with error less than 1%, demonstrating the accuracy of our method for c_1 and c_2 .

We repeat the same procedure to extract c_1 and c_2 coefficients of TF and second- and fourth-order GEAs, which are given by

$$T^{\text{GEA2}} = T^{\text{TF}} + T^{(2)}, \quad (7)$$

and:^{2,17,18}

$$T^{\text{GEA4}} = T^{\text{TF}} + T^{(2)} + T^{(4)}. \quad (8)$$

These gradient corrections to the local approximation are given by

$$T^{(2)} = \frac{5}{27} \int d^3 r r \tau^{\text{TF}}(\mathbf{r}) s^2(\mathbf{r}), \quad (9)$$

and

$$T^{(4)} = \frac{8}{81} \int d^3 r r \tau^{\text{TF}}(\mathbf{r}) \left[q^2(\mathbf{r}) - \frac{9}{8} q(\mathbf{r}) s^2(\mathbf{r}) + \frac{s^4(\mathbf{r})}{3} \right], \quad (10)$$

where $\tau^{\text{TF}}(\mathbf{r})$, $s(\mathbf{r})$, and $q(\mathbf{r})$ are defined as

$$\tau^{\text{TF}}(\mathbf{r}) = \frac{3}{10} k_F^2(\mathbf{r}) n(\mathbf{r}), \quad (11)$$

$$s(\mathbf{r}) = \frac{|\nabla n(\mathbf{r})|}{2k_F(\mathbf{r})n(\mathbf{r})}, \quad (12)$$

$$q(\mathbf{r}) = \frac{\nabla^2 n(\mathbf{r})}{4k_F^2(\mathbf{r})n(\mathbf{r})}, \quad (13)$$

and $k_F(\mathbf{r}) = (3\pi^2 n(\mathbf{r}))^{1/3}$.

We have also applied this procedure to both $T^{(2)}$ and $T^{(4)}$. Since the asymptotic expansions of these energies begin at Z^2 , we extract only a c_1 and a c_2 for each using the following equations:

$$\begin{aligned} \frac{T^{\text{GEA2}} - T^{\text{TF}}}{Z^{7/3}} &= \Delta c_1 Z^{-1/3} + \Delta c_2 Z^{-2/3}, \\ \frac{T^{\text{GEA4}} - T^{\text{GEA2}}}{Z^{7/3}} &= \Delta c_1 Z^{-1/3} + \Delta c_2 Z^{-2/3}. \end{aligned} \quad (14)$$

These results are also included in Table I and are of course consistent with our results from Eq. (6).

IV. RESULTS AND INTERPRETATION

To understand the meaning of the above results, begin with the values of c_1 . We have combined the results of the $T^{(2)}$ and $T^{(4)}$ fits with that of the T^{TF} fit to produce the asymptotic coefficients of T^{GEA2} and T^{GEA4} . We check that these combinations produce the same coefficients in Table I which are found from the direct fitting of T^{GEA2} and T^{GEA4} using Eq. (6). The exact value of c_1 is $-1/2$. We see that the local approximation (TF) gives a good estimate, -0.66 . Then the second-order gradient expansion yields -0.54 , reducing the error by a factor of 5. Finally, the fourth-order

TABLE II. KS kinetic energy (T) in hartrees and various approximations for alkali-earth atoms.

Atom	Z	T_S	T^{TF}	% error	T^{GEA2}	% error	T^{MGEA2}	% error	T^{GEA4}	% error	T^{MGEA4}	% error
Be	4	14.5724	13.1290	-10	14.6471	0.5	15.0880	3.5	14.9854	2.8	14.5453	-0.2
Mg	12	199.612	184.002	-8	198.735	-0.4	203.014	1.7	201.452	0.9	199.924	0.2
Ca	20	676.752	630.064	-7	672.740	-0.6	685.136	1.2	680.286	0.5	677.433	0.1
Sr	38	3131.53	2951.89	-6	3110.44	-0.7	3156.50	0.8	3136.76	0.2	3134.48	0.09
Ba	56	7883.53	7478.27	-5	7829.36	-0.7	7931.34	0.6	7886.19	0.03	7888.14	0.06
Ra	88	23094.3	22065.8	-4	22 945.9	-0.6	23201.5	0.5	23 083.9	-0.05	23 110.5	0.07

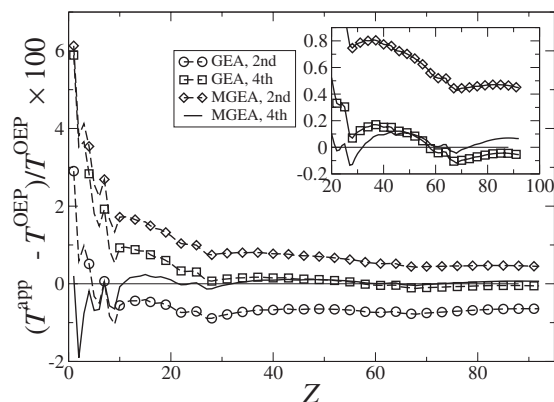


FIG. 3. Percentage errors for atoms (from $Z=1$ to $Z=92$) using various approximations.

gradient expansion yields -0.52 , a further improvement, yielding only a 4% error in its approximation to the Scott correction.¹⁹

For c_2 , the gradient expansion is less useful. The exact result is 0.27 , while the TF approximation overestimates this as 0.39 . The GEA2 result is only slightly reduced (0.34), and the fourth-order correction has the wrong sign.

To understand how important these results can be, we consider how exchange and correlation functionals are constructed. Often, such constructions begin from the GEA, which is then generalized to include (in an approximate way) all powers of a given gradient. For slowly varying densities, it is considered desirable to recover the GEA result. However, we have seen here how this conflicts with the asymptotic expansion, and in Ref. 5, it was shown how the

asymptotic expansion is more significant to energies of real materials and how successful GGAs for atoms and molecules well-approximate the large- Z asymptotic result not the slowly varying gas.

A. Atoms

To illustrate this point, we construct here a trivial modified gradient expansion, MGEA2, designed to have the correct asymptotic coefficients, in so far as is possible. Thus

$$T^{\text{MGEA2}} = T^{\text{TF}} + 1.290T^{(2)}. \quad (15)$$

The enhancement coefficient has been chosen to make $c_1^{\text{MGEA2}} = -1/2$. In Table II, we list the results of several different approximations for the alkali-earth atoms. Because the GEA2 error passes through 0 around $Z=8$, its errors are artificially low.

We can repeat this exercise for the fourth order, matching both c_1 and c_2 to exact values. Now we find:

$$T^{\text{MGEA4}}[n] = T^{\text{TF}}[n] + 1.789T^{(2)}[n] - 3.841T^{(4)}[n], \quad (16)$$

i.e., strongly modified gradient coefficients. This is somewhat arbitrary, as there are several terms in $T^{(4)}$, and there is no real reason to keep their ratios the same as in GEA [Eq. (10)]. However, the results of Table II and Fig. 3 speak for themselves. The resulting functional is better than either GEA for all the alkali earths. Of course, T_S is positive for any density, as are the terms T^{TF} , $T^{(2)}$, and $T^{(4)}$ of the GEA. Equation (16) however can be improperly negative for rapidly varying densities, and so is not suitable for general use.

TABLE III. Noninteracting kinetic energy (in hartrees) for molecules, and errors in approximations. All values are evaluated on the converged KS orbitals and densities obtained with B88-PW91 functionals, and the MGEA4 kinetic energies are evaluated using the TF and the GEA data from Ref. 20.

Atom	T_S^a	T^{TF^a}	T^{GEA2^a}	T^{GEA4^a}	T^{MGEA4}
H	0.500	-0.044	0.011	0.032	-0.026
B	24.548	-2.506	-0.058	0.476	-0.177
C	37.714	-3.731	-0.154	0.600	-0.228
N	54.428	-4.993	-0.097	0.904	-0.078
O	74.867	-6.990	-0.546	0.765	-0.497
F	99.485	-9.093	-0.933	0.659	-0.609
H ₂	1.151	-0.142	-0.014	0.033	-0.094
HF	100.169	-9.016	-0.920	0.639	-0.520
H ₂ O	76.171	-7.074	-0.692	0.565	-0.484
CH ₄	40.317	-3.773	-0.140	0.619	-0.189
NH ₃	56.326	-5.292	-0.400	0.587	-0.331
BF ₃	323.678	-29.052	-2.641	2.454	-1.370
CN	92.573	-8.940	-0.687	0.978	-0.570
CO	112.877	-10.694	-0.911	1.036	-0.670
F ₂	199.023	-18.367	-2.201	0.925	-1.451
HCN	92.982	-8.925	-0.658	1.008	-0.534
N ₂	109.013	-10.487	-0.916	0.999	-0.719
NO	129.563	-12.342	-1.240	0.962	0.279
O ₂	149.834	-14.186	-1.527	0.965	-1.110
O ₃	224.697	-21.636	-2.699	1.028	-2.071
MAE ^b		9.364	0.872	0.812	0.600

^aRef. 20.

^bMean absolute error.

TABLE IV. Jellium surface kinetic energies (erg/cm²) and % error, which is $(\sigma_S^{\text{app}} - \sigma_S^{\text{ex}})/\sigma_S^{\text{ex}}$, of each approximation.

r_s	Exact	T^{TF}	T^{GEA2}	T^{GEA4}	T^{MGEA2} ^a	T^{MGEA4} ^b	T^{LmGGA}
2	-5492.7	11	2.5	1.1	-0.9	0.73	1.3
4	-139.9	54	22	11	12	36	15
6	-3.4	660	330	180	238	675	280

^aSee Eq. (15).^bSee Eq. (16).

B. Molecules

The improvement in total kinetic energies is not just confined to atoms. Also, for noninteracting kinetic energies of molecules, using the data in Ref. 20, Eq. (16) gives a better average of the absolute errors in hartrees (0.6) than T^{TF} (9.4), T^{GEA2} (0.9), and T^{GEA4} (0.8), shown in Table III. Of greater importance are energy differences. For atomization kinetic energies, also using the data in Ref. 20, T^{TF} gives the best averaged absolute error (0.25), which is worsened by gradient corrections. Since the GEA does not have the right quantum corrections from the edges, turning points and Coulomb cores,⁷ GEA does not improve on the atomization process. However, the TF kinetic energy functional is always the dominant term. So, TF gives very good results on the atomization kinetic energies. But the error (0.29) of Eq. (16) is smaller than that of T^{GEA2} (0.36) and T^{GEA4} (0.44). In either case, Eq. (16) works better for atoms and molecules than the fourth-order gradient expansion. Thus, requiring asymptotic exactness is a useful and powerful constraint in functional design.

C. Jellium surfaces

We test this MGEA4 functional for jellium surface kinetic energies. As shown in Table IV, the $T^{(4)}$ term in T^{GEA4} improves the jellium surface kinetic energy in comparison to the results of T^{GEA2} , but Eq. (16) worsens the jellium surface kinetic energies due to the strongly modified coefficient of $T^{(4)}$. This is a confirmation of our general approach. By building in the correct asymptotic behavior for atoms, including the Scott correction coming from the 1s region, we worsen energetics for systems without this feature.

D. Jellium spheres

We also investigate the kinetic energies of neutral jellium spheres (with KS densities using LDA exchange-

correlation and with $r_s=3.9$) from Ref. 21. The analysis of the results is based upon the liquid drop model of Refs. 22 and 23. We write

$$T_S(r_s, N) = \frac{4}{3}\pi R^3 \tau^{\text{unif}}(r_s) + 4\pi R^2 \sigma_S + 2\pi R \gamma_S^{\text{eff}}(r_s, N), \quad (17)$$

where R is the radius of the sphere of uniform positive background. Since we know the bulk (uniform) kinetic energy density τ^{unif} and the surface kinetic energy σ_S for a given functional, we can extract $\gamma_S^{\text{eff}}(r_s, N)$ from this equation, and

$$\lim_{N \rightarrow \infty} \gamma_S^{\text{eff}}(r_s, N) = \gamma_S(r_s) \quad (18)$$

is the curvature energy of jellium. We calculate $\gamma_S^{\text{eff}}(r_s, N)$ using the TF, GEA, MGEA, and a Laplacian-level meta-GGA (LmGGA) of Ref. 21, which is explained further in the following subsection. From Table V, we observe that: (i) gradient corrections in GEA worsen γ_S^{eff} , (ii) the LmGGA of Ref. 21 is even worse than T^{GEA4} , (iii) Eq. (15) (which has the right c_0 and c_1) is not so good, but better than T^{GEA4} , and (iv) Eq. (16) (which has the right c_0 , c_1 , and c_2) gives good results.

E. Existing approximations

We suggest that the large- Z asymptotic expansion is a necessary condition that an accurate kinetic energy functional should satisfy, but is not sufficient. We show this by testing two kinds of semilocal approximations (GGA and meta-GGA) to the kinetic energy functionals.

Recently, Tran and Wesolowski²⁴ constructed a GGA-type kinetic energy functional using the *conjointness conjecture*. They found the enhancement factor by minimizing mean absolute errors of kinetic energies for closed-shell atoms. We evaluate the kinetic energies of atoms using this functional (T^{GGA}) and extract the asymptotic coefficients

TABLE V. $10^4 \times (\gamma_S^{\text{eff}}(\mathbf{r}_S, N) - \gamma_S^{\text{TF}}(\mathbf{r}_S, N))$ in atomic units vs $N=Z$ for neutral jellium spheres with $r_s=3.93$ with various functionals. As $N=Z \rightarrow \infty$, γ_S^{eff} tends to the curvature kinetic energy of jellium, γ_S .

N	Exact	T^{GEA2}	T^{GEA4}	T^{MGEA2} ^a	T^{MGEA4} ^b	T^{LmGGA}
2	-1.8	1.1	2.4	1.5	-2.8	1.9
8	-1.9	1.0	2.1	1.3	-2.3	-5.1
18	-0.5	1.2	2.0	1.6	-0.7	-6.4
58	-0.8	1.3	2.2	1.7	-1.1	-3.2
92	-1.7	1.2	2.0	1.5	-1.0	-1.9
254	-0.5	1.4	2.3	1.8	-0.9	...

^aSee Eq. (15).^bSee Eq. (16).

TABLE VI. KS kinetic energy (T) in hartrees and various approximations for noble atoms.

Atom	Z	T_S	T^{TF}	% error	T^{GEA2}	% error	T^{MGEA2}	% error	T^{GEA4}	% error	T^{MGEA4}	% error
He	2	2.861 68	2.560 51	-11	2.878 47	0.6	2.970 83	3.8	2.962 36	3.5	2.807 17	-1.9
Ne	10	128.545	117.761	-8	127.829	-0.6	130.753	1.7	129.737	0.9	128.447	-0.08
Ar	18	526.812	489.955	-7	524.224	-0.5	534.178	1.4	530.341	0.7	527.772	0.2
Kr	36	2752.04	2591.20	-6	2 733.07	-0.7	2 774.27	0.8	2 756.72	0.2	2754.17	0.08
Xe	54	7232.12	6857.94	-5	7 183.78	-0.7	7 278.42	0.6	7 236.65	0.06	7237.85	0.08
Rn	86	21866.7	20 885.7	-4	2 1725.4	-0.6	21969.3	0.5	21 857.2	-0.04	21881.7	0.07

shown in Table I. This gives a good c_1 coefficient (-0.51), with c_2 (0.29) close to the correct value (0.27), and so is much more accurate than the GEA's.

Perdew and Constantin²¹ constructed a LmGGA for the positive kinetic energy density τ that satisfies the local bound $\tau \geq \tau_W$, where τ_W is the von Weizsäcker kinetic energy density, and tends to τ_W as $r \rightarrow 0$ in an atom. It recovers the fourth-order gradient expansion in the slowly varying limit. We calculate the asymptotic coefficients shown in Table I for this functional. These values are better than those of T^{GEA4} . The good c_1 from T^{GEA4} appears somewhat fortuitous, since there is nothing about a slowly varying density that is relevant to a cusp in the density. The good Scott correction c_1 from the LmGGA comes from correct physics: LmGGA recovers the von Weizsäcker kinetic energy density in the $1s$ cusp, without the spurious but integrable divergences of the integrand of T^{GEA4} .

We finish by discussing other columns of the periodic table. We have also performed all these calculations on the noble gases. In fact, from studies of the asymptotic series,²⁵ it is known that the shell-structure occurs in the next order, $Z^{4/3}$, and that the noble gases are furthest from the asymptotic curves. However, Table VI shows our functionals work almost as well for the noble gas series.

V. MODERN PARAMETRIZATION OF THOMAS-FERMI DENSITY

Our asymptotic expansion study gives new reasons for studying large Z atoms. Our approximate functionals were tested on highly accurate densities, but ultimately, self-consistency is an important and more demanding test. Any approximate functional yields an approximate density via the Euler equation. In this section, we present a new, modern parametrization of the neutral atom TF density, which is more accurate than earlier versions.^{26,27}

The TF density of a neutral atom can be written as

TABLE VII. The values of β_i are found by fitting Eq. (22) to the accurate numerical solution, and those of α_i are the parameters of small- y expansion.²⁸ B is given by 1.588 071 022 6.

α_2	$-B$	β_1	-0.014 405 008 1
α_3	$4/3$	β_2	0.023 142 731 4
α_5	$-2B/5$	β_3	-0.006 177 829 65
α_6	$1/3$	β_4	0.010 319 171 8
α_7	$3B^2/70$	β_5	-0.000 154 797 772
α_8	$-2B/15$		
α_9	$2/27+B^3/252$		

$$n(r) = \frac{Z^2}{4\pi a^3} \left(\frac{\Phi}{x} \right)^{3/2}, \quad (19)$$

where $a = (1/2)(3\pi/4)^{2/3}$ and $x = Z^{1/3}r/a$, and the dimensionless TF differential equation is

$$\frac{d^2\Phi(x)}{dx^2} = \sqrt{\frac{\Phi^3(x)}{x}}, \quad \Phi(x) > 0, \quad (20)$$

which satisfies the following initial conditions:

$$\Phi(0) = 1, \quad \Phi'(0) = -B, \quad B = 1.588\ 071\ 022\ 6. \quad (21)$$

We construct a model for Φ , which recovers the first eight terms of the small- x expansion and the leading term of the asymptotic expansion at large- x ($\Phi(x) \rightarrow 144/x^3$, as $x \rightarrow \infty$). Following Tal and Levy,²⁸ we use $y = \sqrt{x}$ as the variable, because of the singularity of the TF equation. Our parametrization is

$$\Phi^{mod}(y) = \left(1 + \sum_{p=2}^9 \alpha_p y^p \right) / \left(1 + y^9 \sum_{p=1}^5 \beta_p y^p + \frac{\alpha_9 y^{15}}{144} \right), \quad (22)$$

where α_i and β_i are coefficients given in the Table VII. The values of α_i are fixed by the small y -expansion, while those of β_i are found by minimization of the weighted sum of squared residuals χ^2 for $0 < y < 10$. The χ^2 was minimized using the Levenberg-Marquardt method.²⁹ This method is for fitting when the model depends nonlinearly on the set of unknown parameters. 1000 points were used, equally spaced between $y=0$ and $y=10$. We plot the accurate $\Phi(y)$ and our model in Fig. 4, and the differences between them in Fig. 5. These graphs illustrate the accuracy of our parametrization.

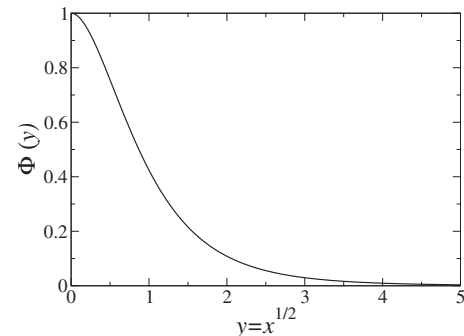


FIG. 4. Accurate numerical $\Phi(y)$ and parametrized $\Phi(y)$ cannot be distinguished.

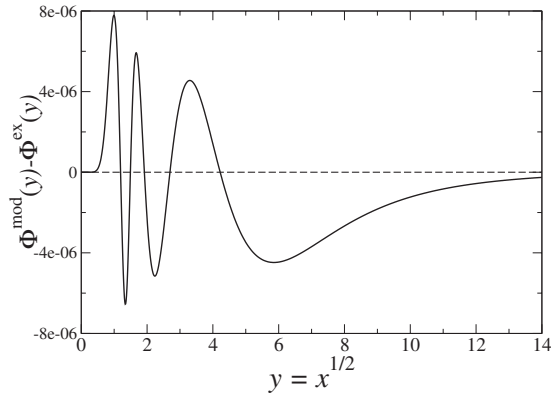


FIG. 5. Errors in the model, relative to numerical integration.

In Table VIII we calculate several moments using our model and existing models that were proposed by Gross and Dreizler²⁶ and Latter.²⁷ The Latter parametrization is

$$\Phi^L(x) = 1/(1 + 0.02747x^{1/2} + 1.243x - 0.1486x^{3/2} + 0.2303x^2 + 0.007298x^{5/2} + 0.006944x^3), \quad (23)$$

and the Gross–Dreizler model (which correctly removes the \sqrt{x} term) is:

$$\Phi^{GD}(x) = 1/(1 + 1.4712x - 0.4973x^{3/2} + 0.3875x^2 + 0.002102x^3). \quad (24)$$

Lastly, we introduce an extremely simple model that we have found useful for pedagogical purposes (even when N differs from Z). We write

$$n^{\text{ped}}(r) = \frac{N}{2\pi^{3/2}R^{3/2}} \frac{1}{r^{3/2}} e^{-r/R}, \quad R = \frac{\alpha N^{2/3}}{Z - \beta N}, \quad (25)$$

where $\alpha = (9/5\sqrt{5})(\sqrt{3}\pi/4)^{1/3}$ and $\beta = 1/2 - 1/\pi$ have been found from integration of the TF kinetic and Hartree energies, respectively, and R minimizes the TF total energy. For $N=Z$, this yields:

$$\Phi^{\text{ped}}(x) = \gamma e^{-2\alpha(1-\beta)x^{3/2}}, \quad \gamma = \frac{5\sqrt{5}}{6\sqrt{3}} \left(\frac{1}{2} + \frac{1}{\pi} \right). \quad (26)$$

This crude approximation does not satisfy the correct initial conditions of Eq. (21),

$$\begin{aligned} \Phi^{\text{ped}}(0) &= \gamma = 0.880361 (\neq 1), \\ \Phi^{\text{ped}'}(0) &= -\frac{125(2+\pi)^2}{648(4\pi^5)^{1/3}} = -0.48 (\neq -1.59). \end{aligned} \quad (27)$$

TABLE VIII. Various moments calculated with our model and with the models of Refs. 26 and 27. Here $M_j^{(p)}$ is given by $\int dx x^p (\Phi(x)/x)^j$.

Moment	Our model	% error	Gross and Dreizler ^a	% error	Latter ^b	% error	$\Phi^{\text{ped}}(x)$	% error	Exact
$M_{3/2}^{(2)}$	0.999857885	-0.01	1.008	0.8	0.999	-0.04	1	0	1
$M_{5/2}^{(2)}$	1.13426462	-0.006	1.1299	-0.4	1.137	0.2	1.11	-2	$5B/7$
$M_2^{(2)}$	0.615438208	0.001	0.6129	-0.4	0.616	0.02	0.72	16	0.615434679 ^c
$M_{3/2}^{(1)}$	1.58799857	-0.005	1.5844	-0.2	1.589	0.07	1.62	2	B

^aReference 26.^bReference 27.^cNumerical result from the TF differential equation.

To compare the quality of the various parametrizations, we calculate the p th moment of the j th power of $\Phi(x)/x$,

$$M_j^{(p)} = \int dx x^p \left(\frac{\Phi(x)}{x} \right)^j. \quad (28)$$

Many quantities of interest can be expressed in terms of these moments.

- (1) Particle number: To ensure $\int d^3r n(\mathbf{r}) = N$, we require

$$M_{3/2}^{(2)} = 1. \quad (29)$$

- (2) TF kinetic energy: The TF kinetic energy is $c_0 Z^{7/3}$, which implies

$$M_{5/2}^{(2)} = \frac{5}{7} B. \quad (30)$$

- (3) The Hartree energy is $U = (1/2) \int \int d^3r d^3r' (n(\mathbf{r})n(\mathbf{r}')/|\mathbf{r} - \mathbf{r}'|) = (1/7a) M_{3/2}^{(1)} Z^{7/3}$, which implies

$$M_{3/2}^{(1)} = B. \quad (31)$$

- (4) The external energy is defined as $V_{\text{ext}} = -\int d^3r Z n(r)/r = -(1/a) M_{3/2}^{(1)} Z^{7/3}$ for the exact TF density, which also implies Eq. (31).

- (5) The LDA exchange energy is defined as $E_X^{\text{LDA}} = A_X \int d\mathbf{r} n^{4/3}(\mathbf{r})$, where $A_X = -(3/4)(3/\pi)^{1/3}$, so for TF, $E_X^{\text{LDA}} = A_X (4\pi a^3)^{(-1/3)} M_2^{(2)} Z^{5/3}$, which implies

$$M_2^{(2)} = 0.615434679, \quad (32)$$

extracted from our accurate numerical solution. LDA exchange suffices^{4,5} for asymptotic exactness to the order displayed in Eqs. (3) and (4); for a numerical study, see Ref. 30.

Table VIII shows that our modern parametrization is far more accurate than existing models by all measures, and that our simple pedagogical model is roughly correct for many features. Finally, we make some comparisons with densities of real atoms to illustrate those features of real atoms that are captured by TF. The radial density $s(\mathbf{r})$ [Eq. (12)] and $q(\mathbf{r})$ [Eq. (13)] are given by

$$4\pi r^2 n(r) = Z^{4/3} f(x)/a, \quad (33)$$

where $f(x) = \sqrt{x} \Phi^{3/2}(x)$,

$$s(r) = \frac{a_1 |g(x)|}{Z^{1/3} f(x)}, \quad a_1 = (9/2\pi)^{1/3}/2, \quad (34)$$

and

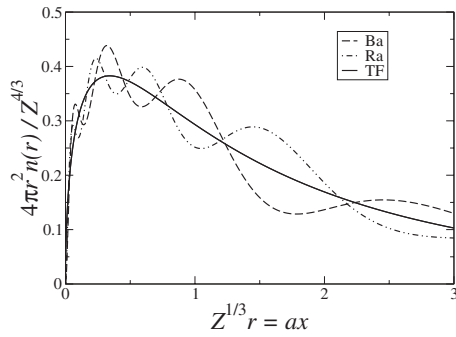


FIG. 6. Plot of the scaled radial densities of Ba and Ra using Eq. (33) and SCF densities. TF scaled densities of Ba and Ra are on top of each other.

$$q(r) = \frac{a_1^2 \{g^2(x) + 2x^2\Phi(x)\Phi''(x)\}}{3Z^{2/3} f^2(x)}, \quad (35)$$

where $g(x)$ is defined as $\Phi(x) - x\Phi'(x)$. The gradient relative to the screening length is

$$t(\mathbf{r}) = \frac{|\nabla n(\mathbf{r})|}{2k_S(\mathbf{r})n(\mathbf{r})}, \quad \text{where } k_S(\mathbf{r}) = \sqrt{4k_F(\mathbf{r})/\pi}, \quad (36)$$

and here

$$t(r) = \frac{a_2 |g(x)|}{(x^3\Phi^5(x))^{1/4}}, \quad a_2 = \frac{3^{5/6}\pi^{1/3}}{2^{8/3}\sqrt{a}} = 0.6124. \quad (37)$$

We also show large- and small- x limit behaviors of various quantities using $\Phi(x) \rightarrow 144/x^3$ as $x \rightarrow \infty$ and $\Phi(x) \rightarrow 1 - Bx + \dots$ as $x \rightarrow 0$.

$$\frac{Z^2}{4\pi a^3} \frac{1}{x^{3/2}} \leftarrow n(r) \rightarrow \frac{432Z^2}{a^3 \pi x^6}, \quad (38)$$

$$\frac{Z^{4/3}}{a} \sqrt{x} \leftarrow 4\pi r^2 n(r) \rightarrow \frac{144Z^{4/3}}{ax^{5/2}}, \quad (39)$$

$$\frac{a_1}{Z^{1/3}} \frac{1}{\sqrt{x}} \leftarrow s(r) \rightarrow \frac{a_1 x}{3Z^{1/3}}, \quad (40)$$

$$\frac{a_1^2}{3Z^{2/3}} \frac{1}{x} \leftarrow q(r) \rightarrow \frac{5a_1^2 x^2}{54Z^{2/3}}, \quad (41)$$

$$\frac{a_2}{x^{3/4}} \leftarrow t(r) \rightarrow \frac{2a_2}{\sqrt{3}}. \quad (42)$$

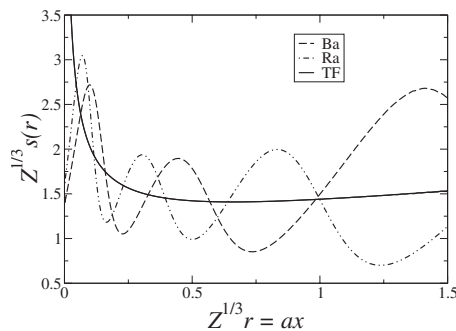


FIG. 7. Plot of the scaled reduced density gradient $s(r)$ (relative to the local Fermi wavelength) vs $Z^{1/3}r$.

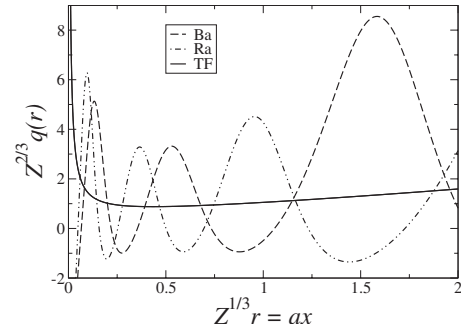


FIG. 8. Plot of the scaled reduced Laplacian $q(r)$ (relative to the local Fermi wavelength) vs $Z^{1/3}r$.

We plot the Z -scaled accurate self-consistent densities and TF radial densities of Ba ($Z=56$) and Ra ($Z=88$) in Fig. 6. Although the shell structure is missing, and the decay at a large distance is wrong, the overall shape of the TF density is relatively correct.

In Figs. 7–9, we plot the scaled $s(r)$, $q(r)$, and $t(r)$ using the self-consistent and TF densities of Ba and Ra. In particular, $t(r)$ measures how fast the density changes on the scale of the TF screening length, and its magnitude does not vary with Z in TF theory. From these figures, we see that $s(r)$, $q(r)$, and $t(r)$ of the TF density diverge near the nucleus, since the TF density does not satisfy Kato's cusp condition.

When $N=Z \rightarrow \infty$ for a realistic density, $s(r)$ is small except in the density tail ($s \sim Z^{-1/3}$ over most of the density), and $q(r)$ is small except in the tail and $1s$ core regions ($q \sim Z^{-2/3}$ over most of the density). This is why gradient expansions for the kinetic and exchange energies, applied to realistic densities, work as well as they do in this limit. The kinetic and exchange energies have only one characteristic length scale, the local Fermi wavelength, but the correlation energy also has a different one, the local screening length. Since $t(r)$ is not and does not become small in this limit, gradient expansions do not work well at all for the correlation energies of atoms.⁵ The standard of “smallness” for s and q , and the more severe standard of smallness for t , are explained in Refs. 5 and 31.

Finally we evaluate $T^{(0)} + T^{(2)}$ on the TF density. We find the correct c_0 in the $Z \rightarrow \infty$ expansion from $T^{(0)}$ but c_1 vanishes, due to the absence of a proper nuclear cusp, and c_2 diverges because $T^{(2)}$ diverges at its lower limit of integration.

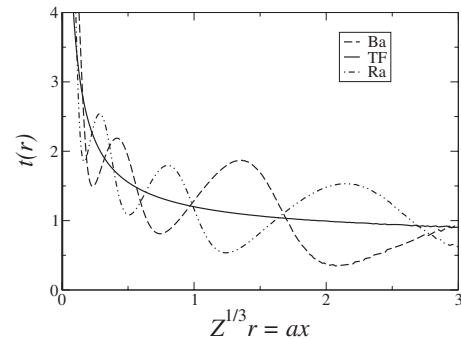


FIG. 9. Plot of the reduced density gradient $t(r)$ (relative to the local screening length) vs $Z^{1/3}r$. As $r \rightarrow \infty$, the TF $t \rightarrow 0.7071$.

VI. SUMMARY

We have shown the importance of the large- N limit for density functional construction of the kinetic energy (with the functional evaluated on a KS density), and also provided a modern, highly accurate parameterization of the neutral-atom TF density. Our results should prove useful in the never-ending search for improved density functionals.

For atoms and molecules, the large- N limit seems more important than the slowly varying limit. On the ladder³² of density-functional approximations, there are three rungs of semilocal approximations (followed by higher rungs of fully nonlocal ones). The LDA uses only the local density, the GGA uses also the density gradient, and the meta-GGA uses in addition the orbital kinetic energy density or the Laplacian of the density. For the exchange-correlation energy, the GGA rung cannot^{5,31} simultaneously describe the slowly varying limit and the $N=Z \rightarrow \infty$ limit for an atom, and we have found here that the same is true (but less severely by percent error of a given energy component) for the kinetic energy. This follows because, as $N=Z \rightarrow \infty$, the reduced gradient $s(r)$ of Eq. (12) becomes small over the energetically important regions of the atom, as can be inferred from Fig. 7, so that a GGA reduces to its own second-order gradient expansion even in regions where a meta-GGA does not⁵ (e.g., near a nucleus, where $q(r)$ diverges but $s(r)$ does not, as shown in Figs. 7 and 8). For the kinetic as for the exchange-correlation energy, meta-GGA's²¹ can recover both the slowly-varying and large- Z limits; it remains to be seen how well fully non-local approximations^{33,34} can do this.

ACKNOWLEDGMENTS

We thank Eberhard Engel for the use of his atomic OPMKS code, and NSF (CHE-0809859 and DMR-0501588) and Korea Science and Engineering Foundation (Grant No. C00063) for support.

¹A *Primer in Density Functional Theory*, edited by C. Fiolhais, F. Nogueira, and M. Marques (Springer-Verlag, New York, 2003).

²R. M. Dreizler and E. K. U. Gross, *Density Functional Theory* (Springer-Verlag, Berlin, 1990).

- ³V.V. Karasiev, R. S. Jones, S. B. Trickey, and F. E. Harris, in *New Developments in Quantum Chemistry*, edited by J. L. Paz and A. J. Hernandez (Research Signpost, Kerala, in press).
- ⁴J. Schwinger, *Phys. Rev. A* **22**, 1827 (1980); F. E. Harris, *ibid.* **24**, 2353 (1981).
- ⁵J. P. Perdew, L. A. Constantin, E. Sagvolden, and K. Burke, *Phys. Rev. Lett.* **97**, 223002 (2006).
- ⁶E. H. Lieb, *Rev. Mod. Phys.* **53**, 603 (1981).
- ⁷P. Elliott, D. Lee, A. Cangi, and K. Burke, *Phys. Rev. Lett.* **100**, 256406 (2008).
- ⁸B.-G. Englert and J. Schwinger, *Phys. Rev. A* **32**, 26 (1985).
- ⁹C. L. Fefferman and L. A. Seco, *Bull. Am. Math. Soc.* **23**, 525 (1990).
- ¹⁰C. L. Fefferman and L. A. Seco, *Adv. Math.* **107**, 1 (1994).
- ¹¹H. Siedentop and R. Weikard, *Commun. Math. Phys.* **112**, 471 (1987).
- ¹²M. Levy and J. P. Perdew, *Phys. Rev. A* **32**, 2010 (1985).
- ¹³E. H. Lieb and B. Simon, *Phys. Rev. Lett.* **31**, 681 (1973).
- ¹⁴E. Engel, OPMKS, atomic DFT program, University of Frankfurt, Germany.
- ¹⁵J. D. Talman and W. F. Shadwick, *Phys. Rev. A* **14**, 36 (1976).
- ¹⁶G. L. Oliver and J. P. Perdew, *Phys. Rev. A* **20**, 397 (1979).
- ¹⁷D. A. Kirzhnits, *Sov. Phys. JETP* **5**, 64 (1957).
- ¹⁸C. H. Hodges, *Can. J. Phys.* **51**, 1428 (1973).
- ¹⁹J. M. C. Scott, *Philos. Mag.* **43**, 859 (1952).
- ²⁰S. S. Iyengar, M. Ernzerhof, S. N. Maximoff, and G. E. Scuseria, *Phys. Rev. A* **63**, 052508 (2001).
- ²¹J. P. Perdew and L. A. Constantin, *Phys. Rev. B* **75**, 155109 (2007).
- ²²J. P. Perdew, Y. Wang, and E. Engel, *Phys. Rev. Lett.* **66**, 508 (1991).
- ²³E. Engel, P. LaRocca, and R. M. Dreizler, *Phys. Rev. B* **49**, 16728 (1994).
- ²⁴F. Tran and T. A. Wesolowski, *Int. J. Quantum Chem.* **89**, 441 (2002).
- ²⁵B.-G. Englert and J. Schwinger, *Phys. Rev. A* **32**, 47 (1985).
- ²⁶E. K. U. Gross and R. M. Dreizler, *Phys. Rev. A* **20**, 1798 (1979).
- ²⁷R. Latter, *Phys. Rev.* **99**, 510 (1955).
- ²⁸Y. Tal and M. Levy, *Phys. Rev. A* **23**, 408 (1981).
- ²⁹*Numerical Recipes in FORTRAN 77*, edited by W. H. Press, B. P. Flannery, S. A. Teukolsky, and W. T. Vetterling (Cambridge University Press, Cambridge, 1992).
- ³⁰S. Kotochigova, Z. H. Levine, E. L. Shirley, M. D. Stiles, and C. W. Clark, *Phys. Rev. A* **55**, 191 (1997); S. Kotochigova, Z. H. Levine, E. L. Shirley, M. D. Stiles, and C. W. Clark, *ibid.* **56**, 5191 (1997).
- ³¹J. P. Perdew, A. Ruzsinszky, G. I. Csonka, O. A. Vydrov, G. E. Scuseria, L. A. Constantin, X. Zhou, and K. Burke, *Phys. Rev. Lett.* **100**, 136406 (2008).
- ³²J. P. Perdew and K. Schmidt, in *Density Functional Theory for Materials*, edited by V. E. Van Doren, K. Van Alsenoy, and P. Geerlings (American Institute of Physics, Melville, 2001).
- ³³Y. A. Wang and E. A. Carter, in *Theoretical Methods in Condensed Phase Chemistry (Progress in Theoretical Chemistry and Physics)*, edited by S. D. Schwartz (Kluwer, Dordrecht, 2000).
- ³⁴D. Garcia-Aldea and J. E. Alvarellos, *Phys. Rev. A* **77**, 022502 (2008).